Check for updates

New Phytologist

Research

Cardiac glycosides protect wormseed wallflower (*Erysimum cheiranthoides*) against some, but not all, glucosinolate-adapted herbivores

Gordon C. Younkin[1,2], Martin L. Alani[1], Anamaría Páez-Capador[1], Hillary D. Fischer[1], Mahdieh Mirzaei[1], Amy P. Hastings[3], Anurag A. Agrawal[3] and Georg Jander[1]

[1]Boyce Thompson Institute, 533 Tower Rd, Ithaca, NY 14853, USA; [2]Plant Biology Section, School of Integrative Plant Science, Cornell University, Ithaca, NY 14853, USA; [3]Department of Ecology and Evolutionary Biology, Cornell University, Ithaca, NY 14853, USA

Author for correspondence:
Georg Jander
Email: gj32@cornell.edu

Received: *21 November 2023*
Accepted: *22 December 2023*

New Phytologist (2024)
doi: 10.1111/nph.19534

Key words: Brassicaceae, *Brevicoryne brassicae*, cardiac glycoside, *Erysimum*, evolution, glucosinolate, herbivory, *Pieris rapae*.

Summary

- The chemical arms race between plants and insects is foundational to the generation and maintenance of biological diversity. We asked how the evolution of a novel defensive compound in an already well-defended plant lineage impacts interactions with diverse herbivores. *Erysimum cheiranthoides* (Brassicaceae), which produces both ancestral glucosinolates and novel cardiac glycosides, served as a model.
- We analyzed gene expression to identify cardiac glycoside biosynthetic enzymes in *E. cheiranthoides* and characterized these enzymes via heterologous expression and CRISPR/Cas9 knockout. Using *E. cheiranthoides* cardiac glycoside-deficient lines, we conducted insect experiments in both the laboratory and field.
- *Ec*CYP87A126 initiates cardiac glycoside biosynthesis via sterol side-chain cleavage, and *Ec*CYP716A418 has a role in cardiac glycoside hydroxylation. In Ec*CYP87A126* knockout lines, cardiac glycoside production was eliminated. Laboratory experiments with these lines revealed that cardiac glycosides were highly effective defenses against two species of glucosinolate-tolerant specialist herbivores, but did not protect against all crucifer-feeding specialist herbivores in the field. Cardiac glycosides had lesser to no effect on two broad generalist herbivores.
- These results begin elucidation of the *E. cheiranthoides* cardiac glycoside biosynthetic pathway and demonstrate *in vivo* that cardiac glycoside production allows *Erysimum* to escape from some, but not all, specialist herbivores.

Introduction

Due to its importance in shaping ecological communities and the species, the chemical arms race between plants and their insect herbivores is a heavily investigated area of molecular ecology (Fraenkel, 1959; Gordon, 1961; Ehrlich & Raven, 1964; Feeny, 1977). Under this paradigm, plants that evolve the ability to produce toxic or deterrent metabolites protect themselves from herbivore feeding and enter a 'new adaptive zone' in which they may rapidly diversify in the absence of natural enemies (Ehrlich & Raven, 1964). However, as their enemies evolve the ability to tolerate or neutralize, these metabolites, they may in turn enter this protected zone (Gordon, 1961), thereby re-applying ecological pressures that force plants to further adapt their defenses.

The Brassicaceae, a family of > 4000 plant species, presents many instances of this chemical arms race between plants and specialized herbivores. Glucosinolates evolved as a defense in this lineage *c.* 90 million years ago and facilitated multiple rounds of species radiations, resulting in the current high species diversity of the Brassicaceae (Edger *et al.*, 2015). Since the original gain of glucosinolate biosynthesis, many insect species have adapted by evolving the ability to tolerate, detoxify, or sequester these compounds (Feeny, 1977; Okamura *et al.*, 2022). Several lineages within the Brassicaceae have more recently evolved the production of additional toxic compounds as a second line of defense: globe candytuft (*Iberis umbellata* L.) makes cucurbitacins (Dong *et al.*, 2021), garlic mustard (*Alliaria petiolata* Bieb.) makes hydroxynitrile glucosides (Frisch & Møller, 2012), scurvy-grass (*Cochlearia* spp. L.) makes tropane alkaloids (Brock *et al.*, 2006), wintercress (*Barbarea vulgaris* W. T. Aiton) makes saponins (Shinoda *et al.*, 2002), and wallflowers (*Erysimum* spp. L.) make cardiac glycosides (cardiac glycosides that inhibit Na^+,K^+-ATPases in animal cells; Makarevich *et al.*, 1994). It is hypothesized that these key evolutionary innovations allowed these lineages to escape their glucosinolate-tolerant specialized herbivores and again diversify (Thompson, 1989; Züst *et al.*, 2020; Dong *et al.*, 2021).

A meta-analysis of phytochemical coevolution theory found that specialist insect herbivores are more sensitive than generalists to compounds that are not found in their typical host plants (Cornell & Hawkins, 2003). Consistent with this theory, the

© 2024 The Authors
New Phytologist © 2024 New Phytologist Foundation

New Phytologist

14698137, 0, Downloaded from https://nph.onlinelibrary.wiley.com/doi/10.1111/nph.19534 by Cornell University, Wiley Online Library on [03/03/2024]. See the Terms and Conditions (https://onlinelibrary.wiley.com/terms-and-conditions) on Wiley Online Library for rules of use; OA articles are governed by the applicable Creative Commons License

glucosinolate-tolerant small and large white cabbage butterflies (*Pieris rapae* L. and *Pieris brassicae* L.) use a wide range of Brassicaceae as host plants but generally avoid *Erysimum*. Experiments involving bioactivity-guided fractionation identified cardiac glycosides as potential agents of this deterrence, and painting cardiac glycosides onto cabbage leaves further established a causal link between the isolated compounds and herbivore behavior (Rothschild *et al.*, 1988; Renwick *et al.*, 1989; Sachdev-Gupta *et al.*, 1993). Similarly, isolated cardiac glycosides were shown to be feeding deterrents for three crucifer-feeding specialist flea beetles (Nielsen, 1978a,b). However, in the absence of mutant lines that lack cardiac glycosides, it has not been possible to conduct *in vivo* tests of the role cardiac glycosides play in *Erysimum*'s escape from herbivory by glucosinolate-tolerant herbivores.

The aims of this study were twofold: First, we sought to identify cardiac glycoside biosynthesis enzymes in wormseed wallflower (*Erysimum cheiranthoides* L.; Fig. 1). Second, we revisited classical ecological experiments with modern tools, developing a protocol for stable transformation of *E. cheiranthoides* and generating CRISPR/Cas9-mediated knockouts of cardiac glycoside biosynthetic genes. This effectively reversed the 'escape from herbivory' of *E. cheiranthoides* and allowed us to directly test the hypothesis that cardiac glycosides in *Erysimum* provide a targeted defense against crucifer-specialist herbivores.

Materials and Methods

Plants, insects, and growth conditions

All experiments were conducted with the genome-sequenced *Erysimum cheiranthoides* L. var. Elbtalaue, which has been inbred for at least eight generations (Züst *et al.*, 2020), Arabidopsis Biological Resource Center (https://abrc.osu.edu) accession no. CS29250. Plants were grown in Cornell Mix (by weight 56% peat moss, 35% vermiculite, 4% lime, 4% Osmocote slow-release fertilizer (Scotts, Marysville, OH, USA), and 1% Unimix (Scotts)) in Conviron (Winnipeg, CA, USA) growth chambers with a 16 h : 8 h photoperiod, 180 μM m^{-2} s^{-1} photosynthetic photon flux density, 60% humidity, and constant 23°C temperature. Once flowering, plants were moved to a climate-controlled glasshouse set to 26°C : 24°C, day : night. Natural light was supplemented with artificial light with a 16 h : 8 h photoperiod.

Cabbage looper (*Trichoplusia ni* Hübner) eggs from Benzon Research (Carlisle, PA, USA) were hatched on an artificial diet (Southland Products, Lake Village, AR, USA) at 28°C. Wild-caught *Pieris rapae* L. butterflies (Ithaca, NY, USA, June 2023) were used to start a laboratory colony. Adults were fed a 10% sucrose solution and were presented with *Brassica oleracea* L. cv capitata for oviposition and caterpillar feeding. Green peach aphids (*Myzus persicae* Sulzer) were from a laboratory colony of a genome-sequenced 'USDA' strain (Ramsey *et al.*, 2007, 2014; Feng *et al.*, 2023). Cabbage aphids (*Brevicoryne brassicae* L.) were from a colony collected in 2015 by Brian Nault (Cornell University) in Geneva, NY, USA. Both aphid species were maintained on *B. oleracea* cv capitata in a growth room with a 16 h : 8 h photoperiod and constant 23°C temperature.

RNA sequencing

Raw RNA sequencing reads from 48 *Erysimum* species (Züst *et al.*, 2020) were downloaded from the NCBI Short Read Archive (PRJNA563696; Strickler *et al.*, 2019). Tissue-specific RNA sequencing data were collected from 6-wk-old wild-type (WT) *E. cheiranthoides* plants, including roots and expanding

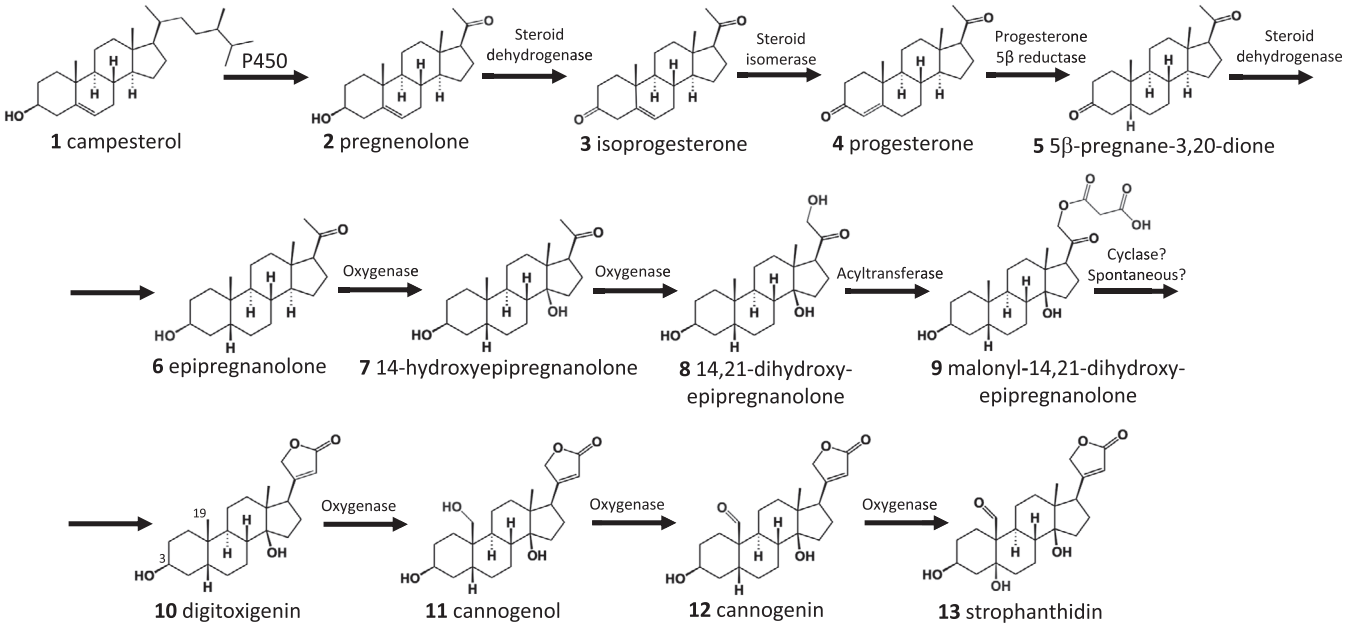

Fig. 1 Proposed *Erysimum cheiranthoides* cardiac glycoside biosynthetic pathway. The first step (sterol side-chain cleavage), and the conversion of digitoxigenin **10** to cannogenol **11** are discussed in this paper. Relevant carbon numbering is shown for digitoxigenin. One or two sugars may be attached at the 3-hydroxyl group.

© 2024 The Authors
New Phytologist © 2024 New Phytologist Foundation

14698137, 0, Downloaded from https://nph.onlinelibrary.wiley.com/doi/10.1111/nph.19534 by Cornell University, Wiley Online Library on [03/03/2024]. See the Terms and Conditions (https://onlinelibrary.wiley.com/terms-and-conditions) on Wiley Online Library for rules of use; OA articles are governed by the applicable Creative Commons License

leaves measuring 1 cm in length (PRJNA1015726). The SV Total RNA Isolation System (Promega Corp., Madison, WI, USA) was employed to isolate total RNA, which was evaluated using a 2100 Bioanalyzer (Agilent Technologies, Santa Clara, CA, USA). Five μg of RNA, pooled from three replicates, was used for the preparation of strand-specific RNA-Seq libraries with 14 cycles of final amplification (Zhong *et al.*, 2011). The libraries were multiplexed and sequenced with a paired-end read length of 150 bp using two lanes on an Illumina HiSeq2500 instrument (Illumina, San Diego, CA, USA) at the Cornell University Biotechnology Resource Center (Ithaca, NY, USA).

Raw RNA sequencing reads for species and tissue datasets were pseudoaligned to the transcriptome associated with *E. cheiranthoides* genome v.2.0 (PRJNA563696; Strickler *et al.*, 2019) using kallisto with default parameters, yielding transcript counts (Bray *et al.*, 2016). Output files were normalized and transformed using the transform_counts.R script from the MR2MODS pipeline (Wisecaver *et al.*, 2017; https://github.itap.purdue.edu/jwisecav/mr2mods). Fold-change expression between leaf and root tissue was calculated using EDGER (Robinson *et al.*, 2010; McCarthy *et al.*, 2012).

Cloning candidate genes

Erysimum cheiranthoides RNA was extracted from 2-wk-old seedlings and young leaves of 5-wk-old plants using the SV Total RNA Isolation System, and cDNA was generated using SMARTScribe Reverse Transcriptase (Takara Bio USA, Ann Arbor, MI, USA). Primers were ordered to include Gateway *attB* recombination sites (Supporting Information Table S1), and the coding sequence was amplified from cDNA using Phusion High-Fidelity DNA Polymerase (New England Biolabs, Ipswich, MA, USA). The gel-purified amplicon was inserted into the pDONR207 vector using Gateway BP Clonase II enzyme mix (Thermo Fisher Scientific, Waltham, MA, USA) and then into pEAQ-HT-DEST1 (Sainsbury *et al.*, 2009) using Gateway LR Clonase II enzyme mix (Thermo Fisher Scientific). The sequences of the inserted genes were verified with Sanger sequencing. All cloning used 10-beta competent *Escherichia coli* (NEB, Ipswich, MA, USA), with heat shock transformation at 42°C. Plasmids were purified using the Wizard Plus SV Miniprep DNA Purification System (Promega Corp.) and transformed into *Agrobacterium tumefaciens* strain GV3101 using a freeze-thaw method (Weigel & Glazebrook, 2006).

Transient expression in *Nicotiana benthamiana*

Genes were transiently expressed in the leaves of 4-wk-old *Nicotiana benthamiana* Domin plants (Bach *et al.*, 2014). A single colony of *A. tumefaciens* strain GV3101 carrying pEAQ-HT-DEST1 containing the candidate gene was inoculated into a 10-ml culture of lysogeny broth, pH 7.5 (LB), with 50 μg ml^{-1} rifampicin, 20 μg ml^{-1} gentamicin, and 50 μg ml^{-1} kanamycin and shaken for 24 h at 28°C and 230 rpm. The bacteria were pelleted for 10 min at 3200 rcf in an Eppendorf Centrifuge 5810 (Hamburg, Germany) and resuspended to $OD_{600} = 0.5$ in 10 mM 2-(N-morpholino) ethanesulfonic acid (MES), 10 mM $MgCl_2$, and 400 μM acetosyringone before resting in the dark for 2 h before infiltration into the abaxial leaf surface using a blunt syringe. Each construct was infiltrated into the leaves of three plants, with pEAQ-HT-DEST1 carrying GFP serving as a negative control. In the case of *Ec*CYP716A418, for which the substrates were not predicted to be present in *N. benthamiana* leaves, a 200 μM solution of digitoxigenin (Sigma-Aldrich) or digitoxin (Sigma-Aldrich) was infiltrated 3 d later. Tissue was collected 5 d after *A. tumefaciens* infiltration for ultrahigh pressure liquid chromatography coupled to mass spectrometry (UPLC–MS) analysis. A 200-μM solution of pregnenolone (Sigma-Aldrich) was infiltrated into separate *N. benthamiana* leaves 2 d before tissue harvest to check for any modifications occurring *in planta*.

gRNA design and CRISPR/Cas9 constructs

One or two CRISPR guide RNAs (gRNAs) were designed to target the first exon of each candidate gene using the IDT CRISPR-Cas9 guide RNA design tool. Single-stranded DNA oligos were ordered for each gRNA, one containing the forward gRNA sequence and a 5′ ATTG, and one containing the reverse complement and a 5′ AAAC (Table S1). Complementary oligos were annealed and inserted into either pARV483 in the case of a single gRNA or into pARV370 in the case of multiple gRNAs targeting the same gene, using Aar1 (New England Biolabs). gRNA cassettes including the AtU6-26 promoter, gRNA scaffold, and AtU6-26 terminator were PCR amplified from pARV370 using primers containing PaqCI (New England Biolabs) restriction sites (Table S1) and inserted in tandem into pARV380 so that all gRNAs targeting the same gene were contained on a single plasmid. Plasmid maps for pARV483, pARV370, and pARV380 are provided in Fig. S1.

Stable transformation of *E. cheiranthoides*

A floral dip stable transformation protocol for *E. cheiranthoides* was developed based on methods previously published for *Arabidopsis thaliana* (L.) Heynh (Clough & Bent, 1998) and *Brassica napus* L. (Wang *et al.*, 2003). *Agrobacterium tumefaciens* strain GV3101 containing a binary plasmid was grown overnight as described above for *N. benthamiana* assays, but the initial 10 ml culture was inoculated into 200 ml fresh LB with the same antibiotics and cultured under the same growth conditions for an additional 24 h.

To prepare the infiltration solution, *A. tumefaciens* cultures were spun down at 3200 rcf in an Eppendorf Centrifuge 5810 for 10 min at room temperature and resuspended in full strength Murashige & Skoog (MS) salts (Research Products International, Mt. Prospect, IL, USA), 50 g l^{-1} sucrose (Sigma-Aldrich), 0.1 mg l^{-1} 6-benzylaminopurine (Sigma-Aldrich), 400 μM acetosyringone (Sigma-Aldrich), and 0.01% Silwet L-77 (PlantMedia.com, Chiang Mai, Thailand) and were allowed to rest for 1 h. The inflorescence of *E. cheiranthoides* plants just beginning to flower was submerged in the bacterial suspension, agitated, and placed under vacuum for 5 min, after which time

© 2024 The Authors
New Phytologist © 2024 New Phytologist Foundation

14698137, 0, Downloaded from https://nph.onlinelibrary.wiley.com/doi/10.1111/nph.19534 by Cornell University, Wiley Online Library on [03/03/2024]. See the Terms and Conditions (https://onlinelibrary.wiley.com/terms-and-conditions) on Wiley Online Library for rules of use; OA articles are governed by the applicable Creative Commons License

the inflorescence was covered with plastic wrap. Plants were kept in the dark for 18–24 h before removing the plastic wrap and transferring to glasshouse conditions. Seeds were harvested 6 wk after dipping. Transformants were identified via *DsRed* fluorescence under an SZX12 stereomicroscope equipped with a UV lamp (Olympus, Center Valley, PA, USA).

Detection of Cas9-induced mutations

T1 plants were screened for mutations using a T7 endonuclease 1 (T7E1) assay. DNA was extracted from 3-wk-old T1 plants by heating a 1 mm leaf disk in 25 µl Extract-N-Amp extraction solution (E7526) at 95°C for 10 min and then adding 25 µl PCR Diluent (E8155; MilliporeSigma, St Louis, MO, USA). Primers were selected to amplify an *c.* 1000 bp region flanking the Cas9 target site (Table S1). PCR was carried out using Phire Green Hot Start II Mastermix (Thermo Fisher Scientific, Waltham, MA, USA) under the manufacturer-recommended conditions. For the T7E1 assay, the Alt-R Genome Editing Detection Kit (Integrated DNA Technologies, Coralville, IA, USA) was used according to manufacturer specifications. In any samples with the presence of non-WT amplicons, PCR products were purified (Wizard SV Gel and PCR Clean-Up System, Promega Corp.) and sent for Sanger sequencing at the Cornell Biotechnology Resource Center (Cornell University, Ithaca, NY, USA). T2 was screened for the absence of fluorescence by microscopy and for the presence of a homozygous mutation at the target site using Sanger sequencing. T3 seeds collected from these T-DNA-free; homozygous mutant plants were used for further analyses.

Metabolite feeding to cyp87a126 *E. cheiranthoides* mutants

Predicted cardiac glycoside intermediates were fed to *cyp87a126-2* mutant plants to check for rescue of cardiac glycoside biosynthesis. Pregnenolone, isoprogesterone (TLC Pharmaceutical Standards, Newmarket, ON, USA), progesterone (Sigma-Aldrich), or 5β-pregnane-3,20-dione (aablocks, San Diego, CA, USA) were suspended to a concentration of 200 µM in 10 mM MES and 10 mM $MgCl_2$ and injected into the abaxial surface of young leaves of 4-wk-old plants. Tissue was collected after 2 d for UPLC–MS analysis.

Metabolite extraction

The same metabolite extraction protocol was used for tissue of both *E. cheiranthoides* and *N. benthamiana*. Two 14 mm leaf disks were collected into a 1.7 ml microcentrifuge tube (Laboratory Products Sales Inc., Rochester, NY, USA), either from an infiltrated region of leaf in the case of infiltration experiments, or from the youngest fully expanded leaves of 4–5-wk-old plants in the case of all other experiments. Tissue was flash frozen in liquid nitrogen and ground with three 3-mm ball bearings (Abbott Ball Co., Hartford, CT, USA) on a 1600 MiniG™ tissue homogenizer (SPEX SamplePrep, Metuchen, NJ, USA). Metabolites were extracted in 100 µl 70% methanol containing 15 µM internal standard (ouabain for positive ionization mode, sinigrin for negative ionization mode). Samples were vortexed to suspend the plant tissue and left to extract for half an hour at room temperature before being centrifuged twice for 10 min at 17 000 rcf in a Z207-M microcentrifuge (Hermle, Sayreville, NJ, USA), transferring to a clean tube before the second centrifugation.

Ultrahigh pressure liquid chromatography coupled to mass spectrometry

Plant extracts were analyzed on an UltiMate 3000 UHPLC system coupled to a Q-Exactive hybrid quadrupole-orbitrap mass spectrometer (Thermo Fisher Scientific). The instrument was fitted with a Supelco Titan™ C18 UHPLC Column (80 Å, 100 × 2.1 mm, particle size 1.9 µm; Sigma-Aldrich). Two-µL injections were separated using a short (for quantification) or long (for figures) solvent gradient. Mobile phases were A: water +0.1% (v/v) formic acid, and B: acetonitrile +0.1% (v/v) formic acid, all Optima LC/MS grade (Thermo Fisher Scientific). Short gradient: 0–0.5 min, hold at 2% B; 0.5–10 min, linear gradient from 2% to 97% B; 10–11.5 minutes, hold at 97% B, 11.5–13 min, hold at 2% B. Long gradient: 0–5 min, hold at 2% B; 5–22 min, linear gradient from 2% to 97% B; 22–23.5 min, hold at 97% B, 23.5–25 min, hold at 2% B. The solvent flow rate was 0.5 ml min^{-1}, the column oven 40°C, and the autosampler temperature 15°C. Mass spectrometry data were acquired in positive ionization mode for the detection of cardiac glycosides and negative ionization mode for the detection of glucosinolates in full scan mode from *m/z* 150 to 900. The following settings were used: capillary voltage 3.5 kV (positive mode) or 3.0 kV (negative mode), capillary temperature 380°C, sheath gas 60, auxiliary gas 20, and S-Lens RF level 50.

LCMS data processing

LC-MS peak areas were quantified using a custom processing method in XCALIBUR™ Software (Thermo Fisher Scientific) using the following parameters: peak detection ICIS, smoothing points 1, baseline window 40, area noise factor 5, peak noise factor 15, and tailing factor 2. Mass features used for quantification are provided in Table S2 for cardiac glycosides and Table S3 for glucosinolates.

Na^+,K^+-ATPase inhibition assay

The inhibitory effect of plant extracts on porcine (*Sus scrofa* L) Na^+,K^+-ATPase was measured following the protocol described in Petschenka *et al.* (2023). Two biological replicates of WT *E. cheiranthoides* (each with two technical replicates) and four biological replicates of *cyp87a126-1*, *cyp87a126-2*, and *A. thaliana* (each with one technical replicate) were assayed. Using the enzymatic activity across sample dilutions, sigmoid dose–response curves were calculated using a logistic function in the NLME package (Pinheiro & Bates, 2000, 2023) in R statistical software (R Core Team, 2020). For each sample, the relative dilution at the inflection point was calculated to estimate the half-maximal inhibitory concentration (IC50).

© 2024 The Authors
New Phytologist © 2024 New Phytologist Foundation

14698137, 0, Downloaded from https://nph.onlinelibrary.wiley.com/doi/10.1111/nph.19534 by Cornell University, Wiley Online Library on [03/03/2024]. See the Terms and Conditions (https://onlinelibrary.wiley.com/terms-and-conditions) on Wiley Online Library for rules of use; OA articles are governed by the applicable Creative Commons License

Insect bioassays

For caterpillar growth and survival assays, individual 2-d-old *T. ni* or *P. rapae* larvae were restricted to a single leaf of 4-wk-old *E. cheiranthoides* WT, *cyp87a126-1*, and *cyp87a126-2* mutant lines (Fig. S2) using 6.5 × 8 cm organza bags (amazon.com, item B073J4RS9C). For *T. ni*, 12 plants were used for each line, and caterpillars were placed on five leaves of each plant for a total of 60 caterpillars per line. Some caterpillars were removed due to underwatering of plants or caterpillar death/escape (WT: 37 caterpillars removed, *cyp87a126-1*: 25, *cyp87a126-2*: 32). For *P. rapae*, a variable number of plants per line was used (WT: 14 plants, *cyp87a126-1*: 17 plants, *cyp87a126-2*: 13 plants), with one caterpillar on a single leaf of the same age per plant. After 8 d, leaf damage was assessed, and surviving larvae were moved to a fresh leaf to continue feeding.

Aphid and caterpillar choice assays were conducted in 100 × 15 mm Petri dishes (Thermo Fisher Scientific) sealed with Parafilm. For *T. ni*, 14 mm leaf disks from young leaves were placed in pairs of one WT and one mutant leaf disk on wet paper towels along with a single neonate caterpillar, with 20 replicates per mutant line (Fig. S2). After 48 h, photographs were taken of each leaf disk, and leaf area eaten was quantified using the Leaf Byte app (Getman-Pickering *et al.*, 2020). Two replicates for each line were removed due to desiccation. For *M. persicae* and *B. brassicae*, detached leaves were used instead of leaf disks, and 10 adult aphids were placed in each Petri dish (Fig. S2). Twelve replicates were assayed for each mutant line, and after 24 h, the number of aphids on each leaf was recorded. Replicates suffering from desiccation were removed (*M. persicae*: two replicates removed for each line, *B. brassicae*: three removed for *cyp87a126-1*, one removed for *cyp87a126-2*).

Myzus persicae and *B. brassicae* colony growth was measured by transferring five adult aphids from cabbage to bagged 3-wk-old *E. cheiranthoides* plants, with 12 replicates for WT and each mutant line. After 9 d, the combined number of adults and nymphs was recorded for each plant.

Pieris rapae oviposition assays were conducted using laboratory-reared adult butterflies. One WT plant and one mutant plant (either *cyp87a126-1* or *cyp87a126-2*) were placed in a 38 × 38 × 60 cm mesh cage with a mating pair of *P. rapae* butterflies and a 10% sucrose solution (Fig. S2). Butterflies were monitored daily and the total number of eggs on each plant was recorded once the female butterfly died or after 5 d. There were 11 replicates for each mutant line, but many butterflies died before laying any eggs, leaving only six replicates for *cyp87a126-1* and four replicates for *cyp87a126-2*. Because *P. rapae* lay eggs one at a time and not in clusters, replicates were pooled and the overall distribution of eggs between WT and mutant lines was used for statistical analysis.

Field experiment

Three-week-old *E. cheiranthoides* plants were transplanted to a freshly plowed field in Ithaca, NY, USA, on 31 July 2023. Plants were arranged in blocks of six, with each block containing two WT plants, one plant each from *cyp87a126-1* and *cyp87a126-2* mutant lines, and two plants from glucosinolate knockdown lines that are otherwise not discussed in this study. Each block was arranged in a 2 × 3 pattern, with genotypes randomized within each block, and plants spaced 40 cm apart. There were three rows of 10 blocks spaced 1.1 m apart on all sides, for a total of 30 blocks and 180 plants. There was a 2-m buffer on all sides between the experimental plot and unplowed areas. Visitors to each plant were recorded during four separate censuses over the course of a month and visually identified to the lowest possible taxon. Plants that died before the end of the experiment or that were cut down at ground level by a suspected mammalian herbivore were removed, leaving 52 WT, 27 *cyp87a126-1*, and 24 *cyp87a126-2* plants. Only taxa found on at least 25 plants (> 24% of surviving plants) across the course of the experiment were retained for statistical analysis.

Statistical analysis

All statistical analyses were carried out in R statistical software (R Core Team, 2020). The following functions and packages were used: EDGER (Robinson *et al.*, 2010; McCarthy *et al.*, 2012) for differential gene expression analysis, aov, and TukeyHSD for one-way ANOVA and *post hoc* Tukey's HSD for most metabolite abundance and insect assays. A Kruskal–Wallis test (kruskal.test) with pairwise Wilcoxon *post hoc* tests (pairwise.wilcox.test) were used for the non-normally distributed results of the *B. brassicae* colony growth assay. For analysis of results from the field experiment, a generalized linear model with a binomial distribution was fitted to the presence/absence of each visitor on a given plant across all four censuses using glm. In the case of a significant genotype effect, pairwise contrasts and Tukey-adjusted *P*-values were estimated using EMMEANS (Lenth, 2023). *Phyllotreta striolata* (F.) was found on every plant, so a model based on presence/absence was not informative. Instead, a one-way ANOVA (aov function in R) was performed on counts of *P. striolata* beetles per plant. Plots were made using the packages GENEMODEL (Monroe, 2017), MSNBASE (Gatto & Lilley, 2012; Gatto *et al.*, 2020), and MULTCOMPVIEW (Graves *et al.*, 2023). R scripts for all statistical analyses are available on GitHub (https://github.com/gordonyounkin/EcCYP87A126_scripts), and raw data underlying all figures are available in the Supporting Information.

Phylogenetic inference

Homologous proteins with at least 70% amino acid sequence identity to the candidate enzymes were identified from selected species using BLAST against public databases. For each candidate, an *A. thaliana* cytochrome P450 with between 35% and 50% amino acid identity was selected as an outgroup. Protein sequences were aligned using CLUSTALW (Sievers *et al.*, 2011; Madeira *et al.*, 2022), and phylogenies were inferred using IQ-TREE web server (Trifinopoulos *et al.*, 2016; Hoang *et al.*, 2018; Minh *et al.*, 2020) with default parameters, except the number of bootstrap alignments was increased to 10 000.

© 2024 The Authors
New Phytologist © 2024 New Phytologist Foundation

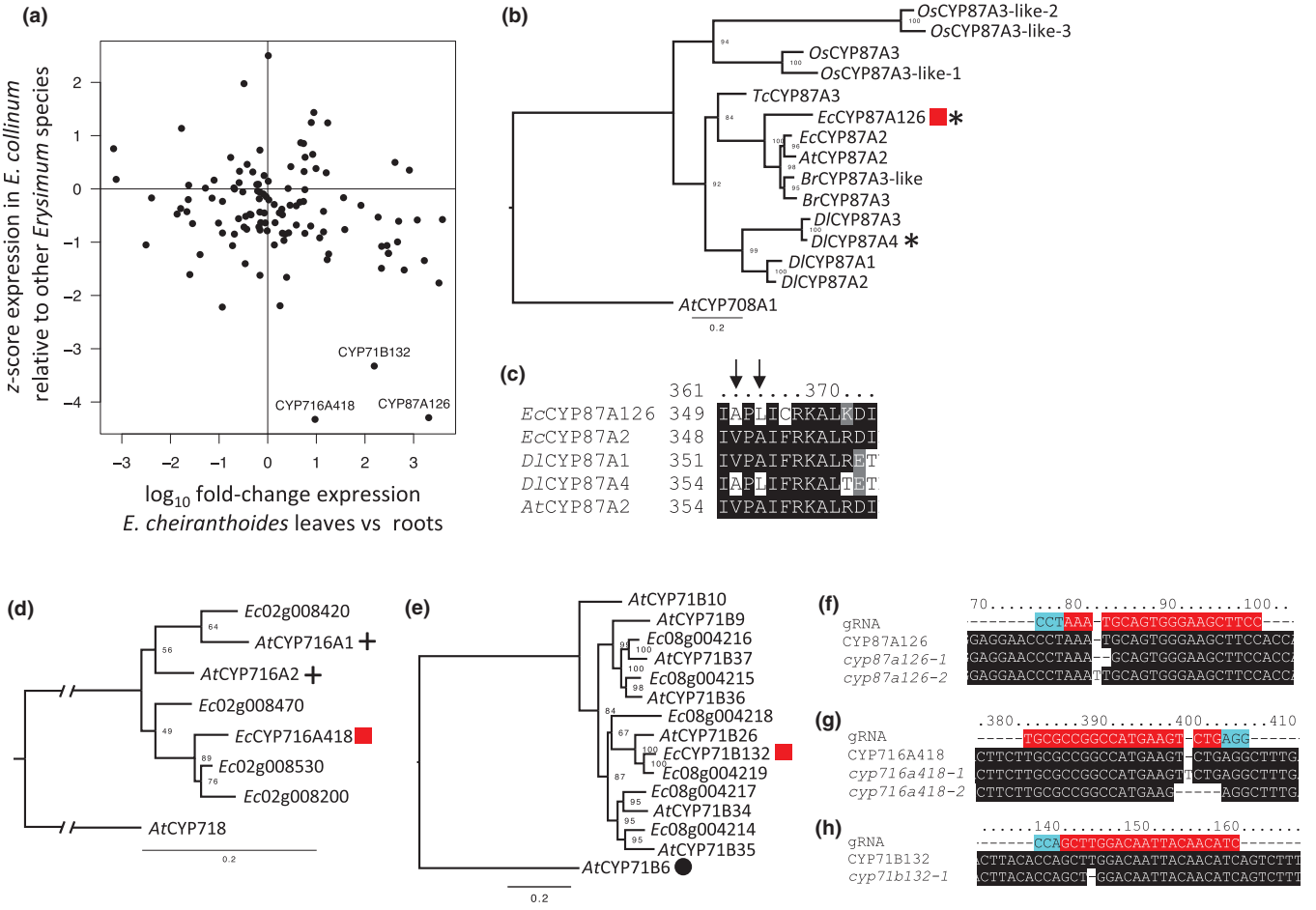

Fig. 2 Identification and knockout of candidate cytochrome P450s. (a) Expression pattern of cytochrome P450 monooxygenases in *Erysimum cheiranthoides*. Fold change in expression between young leaves and roots is plotted against *z*-score of expression in *E. collinum* relative to 48 *Erysimum* species. Genes with high expression in young leaves, where cardiac glycosides are synthesized, and low expression in *E. collinum*, which does not produce cardiac glycosides, are good candidates for involvement in cardiac glycoside biosynthesis. (b, d, e) Gene trees of candidate cytochrome P450s. Species abbreviations: *At*, *Arabidopsis thaliana*; *Br*, *Brassica rapa*; *Dl*, *Digitalis lanata*; *Ec*, *Erysimum cheiranthoides*; *Os*, *Oryza sativa*; *Tc*, *Theobroma cacao*. Candidate genes are marked with a red square. Genes encoding enzymes with known activity or substrates are marked with a black star (*, sterol side-chain cleaving), black plus (triterpenoid hydroxylation), and black circle (indolic compounds). Bootstrap support is indicated for each node, and scale bars represent expected number of nucleotide substitutions per site. (c) Alignment of selected CYP87A proteins. Convergent amino acid substitutions that are critical for sterol side-chain cleaving activity are marked with an arrow. (f–h) Location and sequence of Cas9 protospacers (red, with 3′ NGG PAM in turquoise) used for generation of mutant lines with wildtype and mutant sequences. A number of basepairs from the start of the coding sequence are indicated.

Results

Identification of candidate genes

To identify cytochrome P450 monooxygenases involved in cardiac glycoside biosynthesis, we examined patterns of gene expression across *E. cheiranthoides* tissues and between 48 different species in the genus *Erysimum*. Two criteria were used as follows: (1) High expression in leaves of *E. cheiranthoides* relative to roots, as grafting experiments showed that cardiac glycosides are synthesized in leaves and transported to the roots (Alani *et al.*, 2021). (2) Lower expression in *Erysimum collinum* (M.Bieb.) Andrz. ex DC. relative to all other species of *Erysimum*, because *E. collinum* produces nearly undetectable levels of cardiac glycosides (Züst *et al.*, 2020). Of 116 cytochrome P450s across the two expression datasets, three matched both criteria, with at least ninefold greater expression in young leaves relative to roots, and expression in *E. collinum* leaves > three standard deviations below the mean of expression levels in other *Erysimum* species (Fig. 2a). These three cytochrome P450s, *Ec*CYP71B132, *Ec*CYP716A418, and *Ec*CYP87A126, were selected as candidates for involvement in cardiac glycoside biosynthesis. Full-length coding sequences are provided in Table S4.

Phylogenetic analysis of candidate genes

The three candidate genes are from distinct cytochrome P450 families, sharing no more than 26% amino acid sequence identity

© 2024 The Authors
New Phytologist © 2024 New Phytologist Foundation

14698137, 0, Downloaded from https://nph.onlinelibrary.wiley.com/doi/10.1111/nph.19534 by Cornell University, Wiley Online Library on [03/03/2024]. See the Terms and Conditions (https://onlinelibrary.wiley.com/terms-and-conditions) on Wiley Online Library for rules of use; OA articles are governed by the applicable Creative Commons License

14698137, 0, Downloaded from https://nph.onlinelibrary.wiley.com/doi/10.1111/nph.19534 by Cornell University, Wiley Online Library on [03/03/2024]. See the Terms and Conditions (https://onlinelibrary.wiley.com/terms-and-conditions) on Wiley Online Library for rules of use; OA articles are governed by the applicable Creative Commons License

with one another. However, all three are in clades containing duplication events relative to *A. thaliana* (Fig. 2b,d,e). *Ec*CYP87A126 is of particular interest because of recent reports identifying CYP87A members as capable of sterol side-chain cleavage in several species including woolly foxglove (*Digitalis lanata* Ehrh.; Carroll *et al.*, 2023), common foxglove (*D. purpurea* L.), Sodom apple (*Calotropis procera* W. T. Aiton), and *E. cheiranthoides* (Kunert *et al.*, 2023). To better understand the convergence of this activity in diverse lineages, we aligned the amino acid sequences of *Ec*CYP87A126 and *Dl*CYP87A4. We found that the two amino acid substitutions identified by Carroll *et al.* (2023) as necessary for sterol side-chain cleaving activity, V355A and A357L in *Dl*CYP87A4, were also present in *Ec*CYP87A126 (Fig. 2c). *Ec*CYP716A418 is also a promising candidate enzyme, as closely related enzymes from *A. thaliana*, *At*CYP716A1, and *At*CYP716A2, act on triterpenoids (Yasumoto *et al.*, 2016), which are structurally related to cardiac glycosides. Whereas *Ec*CYP71B132 is not related to known triterpenoid-modifying proteins, its corresponding gene expression pattern was compelling enough to continue pursuing it as a candidate.

Cardiac glycoside content is altered in Cas9-generated cyp87a126 and cyp716a418 mutant lines

We generated independent knockout lines for each of the three cytochrome P450s using Cas9-mediated gene editing (Figs 2f–h, S3). The knockout lines did not display an obvious visual phenotype (Fig. 3b), and the Ec*CYP71B132* knockout line displayed no changes in cardiac glycoside content (Fig. 3a). Knockout lines for the other two candidate genes had strong alterations in cardiac glycoside accumulation. Ec*CYP716A418* knockouts hyperaccumulate glycosides of digitoxigenin (**10**) (Fig. 3a,d; Table S5, one-way ANOVA: $F_{2,10} = 74.01$, $P < 0.001$; Tukey's HSD: WT-*cyp716a418-1* $P < 0.001$, WT-*cyp716a418-2* $P < 0.001$), apparently lacking the ability to hydroxylate digitoxigenin at carbon 19 to form cannogenol (**11**), cannogenin (**12**), and strophanthidin (**13**) (Fig. 1). Ec*CYP87A126* knockout lines accumulated barely detectable levels of cardiac glycosides (Fig. 3a), suggesting that it is an essential enzyme in cardiac glycoside biosynthesis. Despite a 1000-fold decrease in total cardiac glycoside-related peak area (Fig. 3c; Table S6, one-way ANOVA: $F_{2,12} = 271$, $P < 0.001$; Tukey's HSD: WT-*cyp87a126-1* $P < 0.001$, WT-*cyp87a126-2* $P < 0.001$), *cyp87a126* lines display no difference in aliphatic (one-way ANOVA: $F_{2,10} = 2.32$, $P = 0.15$) or indole (one-way ANOVA: $F_{2,10} = 1.71$, $P = 0.23$) glucosinolate abundance (Fig. 3c; Table S7).

Transient expression of *E. cheiranthoides* cytochrome P450s in *N. benthamiana* leaves

To investigate the enzymatic activity of *Ec*CYP716A418 and *Ec*CYP87A126, full-length coding sequences were cloned and transiently expressed in *N. benthamiana* leaves, with substrate co-infiltration where necessary. Based on the strong phenotype of the knockout lines, we expected *Ec*CYP716A418 to hydroxylate digitoxigenin at carbon 19. However, no activity was detected upon co-infiltration with digitoxigenin or digitoxin, a glycosylated form of digitoxigenin. *Nicotiana benthamiana* leaves expressing *Ec*CYP87A126 accumulated pregnenolone (**2**), consistent with previous studies showing that some members of the CYP87A family possess sterol side-chain cleaving activity (Fig. 3e,f; Carroll *et al.*, 2023; Kunert *et al.*, 2023).

Using cyp87a126 mutant lines to investigate intermediates in cardiac glycoside biosynthesis

cyp87a126 mutant lines provide a tool for investigation of intermediates in cardiac glycoside biosynthesis, as only the first enzyme in the pathway is absent and the rest of the pathway remains intact. The following predicted intermediates were fed to *cyp87a126-2* plants: pregnenolone (**2**), isoprogesterone (**3**), progesterone (**4**), and 5β-pregnane-3,20-dione (**5**). All infiltrated substrates rescued cardiac glycoside biosynthesis in *cyp87a126-2* plants (Fig. 4), consistent with the pathway shown in Fig. 1.

Leaf extracts of cyp87a126 mutant lines display decreased Na^+,K^+-ATPase inhibition

Cardiac glycosides are strong inhibitors of Na^+,K^+-ATPase activity in animals (Petschenka *et al.*, 2023). Therefore, we assessed the *cyp87a126* mutant lines for Na^+,K^+-ATPase inhibitory activity using an *in vitro* assay with porcine Na^+,K^+-ATPase. Methanolic extracts of *cyp87a126-1* displayed on average 15-fold lower inhibitory activity than extracts of WT leaves, and *cyp87a126-2* showed 251-fold lower inhibitory activity, on par with the cardiac glycoside-free *A. thaliana* control (Fig. 5a,b; Table S8). A one-way ANOVA on log-transformed half-maximal inhibitory concentration (IC50) data found differences between WT and both *cyp87a126* lines (one-way ANOVA, $F_{3,12} = 69.34$, $P < 0.001$; Tukey's HSD: WT-*cyp87a126-1* $P < 0.001$, WT-*cyp87a126-2* $P < 0.001$, *cyp87a126-1*-*cyp87a126-2* $P = 0.051$). Although we see some apparent Na^+,K^+-inhibition at high concentrations of both *A. thaliana* and cardiac glycoside-free *E. cheiranthoides* lines, this likely is an artefact of the assay. High concentrations of plant extract can interfere with spectrophotometric measurements or cause nonspecific inhibition by interacting with assay components. This makes it difficult to quantify the decrease in inhibitory activity that can be attributed solely to cardenolides.

Insect performance on cyp87a126 mutant lines

To test the impact of cardiac glycosides on insects feeding on *E. cheiranthoides*, we conducted insect choice and performance assays using two generalist herbivores, *M. persicae* and *T. ni*, and two crucifer-feeding specialists, *B. brassicae* and *P. rapae*. In choice assays, the overall trend was a preference for cardiac glycoside-free mutant lines, with varying levels of significance for each species. While more adult *M. persicae* aphids chose mutant lines over WT (*cyp87a126-1*: 56% chose mutant, *cyp87a126-2*: 67% chose mutant), this difference was not significant (Fig. 5c;

© 2024 The Authors
New Phytologist © 2024 New Phytologist Foundation

New Phytologist

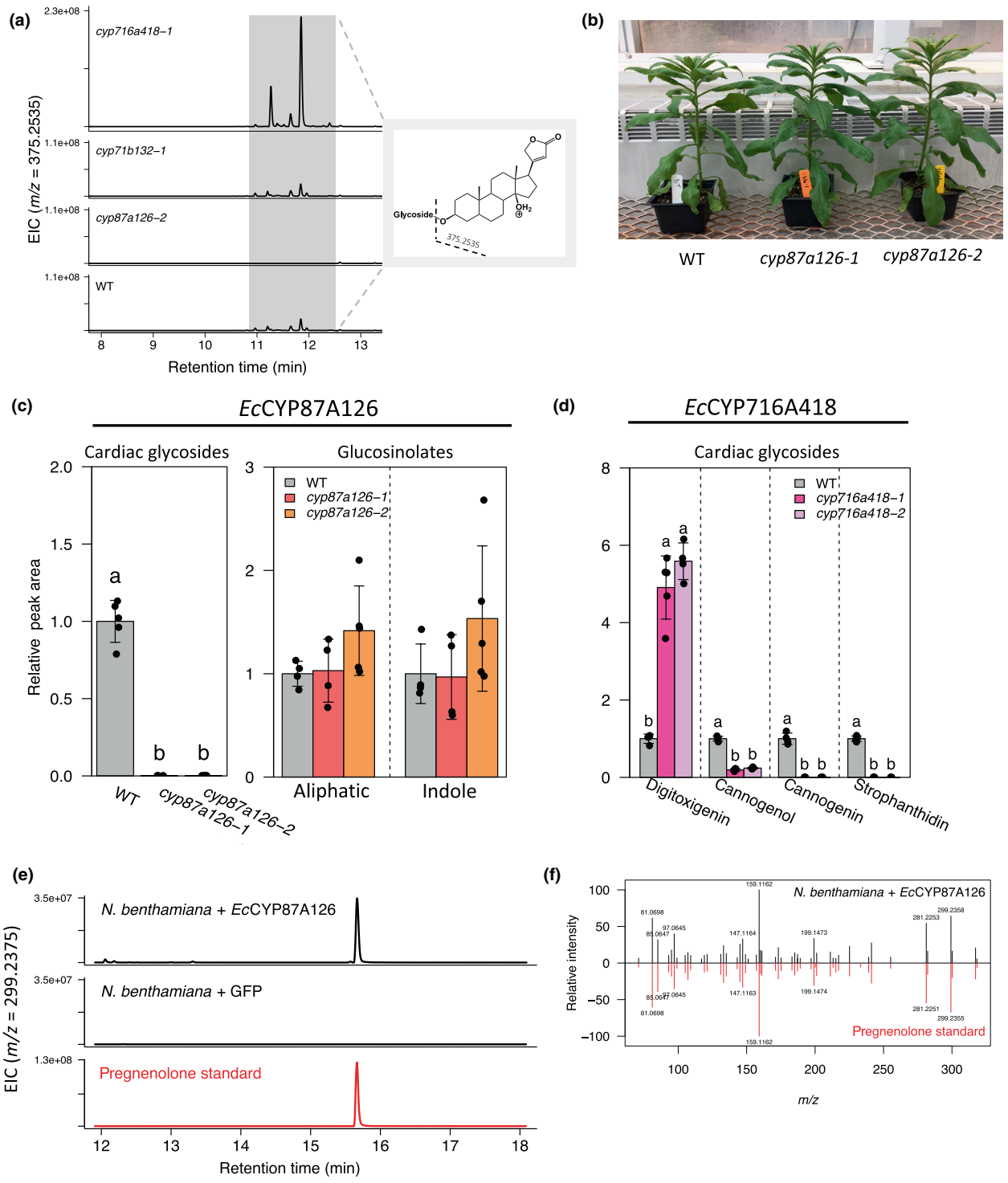

Fig. 3 *Erysimum cheiranthoides* Ec*CYP87A126* and Ec*CYP716A418* mutant lines have altered cardiac glycoside content. (a) Extracted ion chromatograms from a representative mutant plant for each candidate gene. $m/z = 375.2535$ is a fragment common to all digitoxigenin-containing cardiac glycosides in positive electrospray ionization. (b) Despite lacking cardiac glycosides, *cyp87a126* mutant plants show no obvious growth phenotype. (c) Total cardiac glycoside and glucosinolate-related peak area in *cyp87a126* mutants compared with wildtype (WT). (d) Cardiac glycoside abundance by genin in *cyp716a418* mutant lines compared with WT. For all plots, error bars indicate ±SD ($n = 4$–5); letters indicate statistical differences ($P < 0.001$) according to a one-way ANOVA followed by Tukey's HSD. $n = 4$–5 plants per line. (e) Extracted ion chromatograms ($m/z = 299.2375$, pregnenolone $[M\text{-}H_2O + H]^+$) of *Nicotiana benthamiana* leaves expressing EcCYP87A126 or a GFP control. A pregnenolone standard (red) was infiltrated into a separate *N. benthamiana* leaf to account for any potential modifications made by endogenous enzymes. (f) MSMS spectra isolated from $m/z = 315.2324$ (pregnenolone $[M + H]^+$) for pregnenolone standard (red) compared with product of *Ec*CYP87A126 (black).

© 2024 The Authors
New Phytologist © 2024 New Phytologist Foundation

14698137, 0, Downloaded from https://nph.onlinelibrary.wiley.com/doi/10.1111/nph.19534 by Cornell University, Wiley Online Library on [03/03/2024]. See the Terms and Conditions (https://onlinelibrary.wiley.com/terms-and-conditions) on Wiley Online Library for rules of use; OA articles are governed by the applicable Creative Commons License

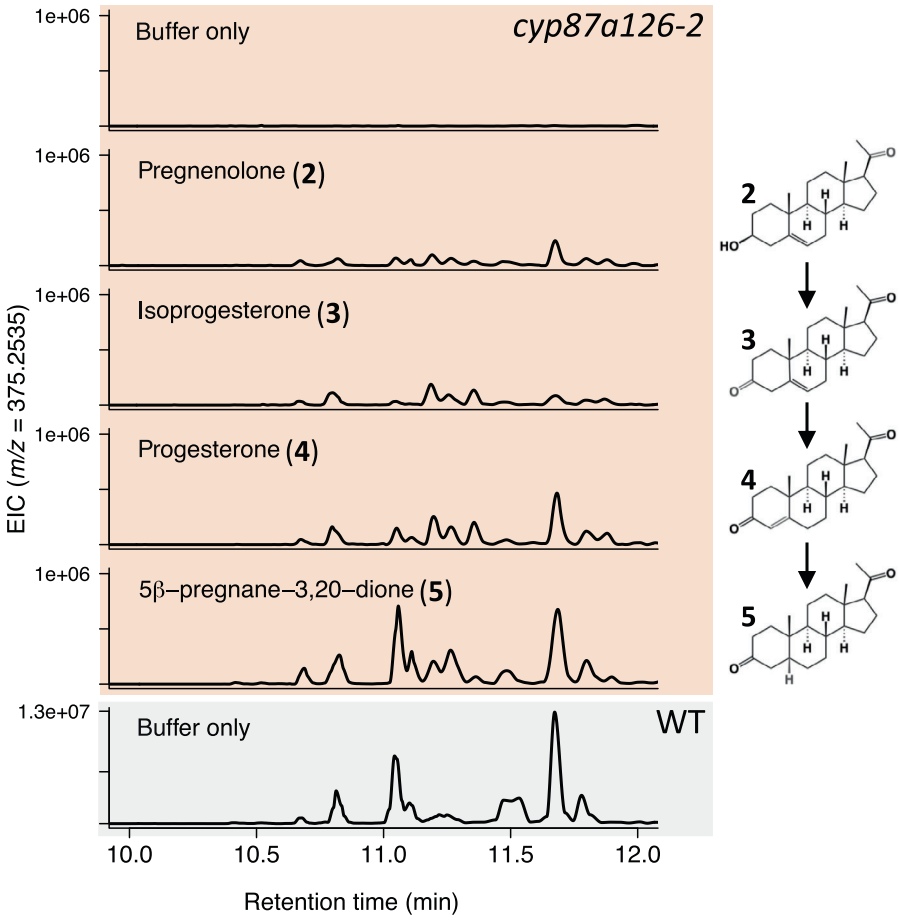

Fig. 4 Rescue of cardiac glycoside biosynthesis in the *Ersyimum cheiranthoides cyp87a126-2* mutant line. ESI+ extracted ion chromatograms of $m/z = 375.2535$, a fragment that arises from digitoxigenin glycosides in positive ionization mode corresponding to the loss of all sugar moities. *cyp87a126-2* plants 2 d after infiltration of predicted intermediates (orange background) are compared with wildtype (grey background).

Table S9, paired *t*-test: *cyp87a126-1* $P = 0.12$, *cyp87a126-2*: $P = 0.08$). *Trichoplusia ni* caterpillars showed a clear preference for *cyp87a126* mutant lines over WT, as measured by leaf area eaten (Figs 5d, S4; Table S10; paired *t*-test: *cyp87a126-1* $P = 0.001$, *cyp87a126-2* $P = 0.013$). Similarly, adult *B. brassicae* aphids displayed a strong preference for cardiac glycoside-free mutant lines (Fig. 5e; Table S11; paired *t*-test: *cyp87a126-1* $P = 0.004$, *cyp87a126-2*: $P = 0.009$). Gravid adult *P. rapae* almost exclusively chose to oviposit on *cyp87a126* mutant plants, with all 128 eggs were laid on mutant plants for *cyp87a126-1* ($\chi^2 = 128$, df = 1, $P < 0.001$), and 74 of 75 eggs were laid on mutant plants for *cyp87a126-2*, with only one egg laid on WT ($\chi^2 = 71.1$, df = 1, $P < 0.001$; Fig. 5f; Table S12).

Results were less uniform in performance assays. For *M. persicae*, population growth over 9 d from five adult aphids restricted to a single plant was not different between WT and either mutant line (Fig. 5c; Table S13; one-way ANOVA: $F_{2,33} = 0.27$, $P = 0.77$). When bagged on individual leaves, *T. ni* was more likely to refuse to feed on WT than on either mutant line (Fig. 5d; $\chi^2 = 17.44$, df = 2, $P < 0.001$). Caterpillars that did begin feeding grew marginally better on *cyp87a126-1* than on WT after correcting for leaf age, but there was no difference between *cyp87a126-2* and WT (Fig. 5d; Table S14; one-way ANOVA $F_{2,82} = 4.18$, $P = 0.019$, Tukey's HSD: WT-*cyp87a126-1* $P = 0.014$, WT-*cyp87a126-2* $P = 0.22$). Adult *B. brassicae* aphids were unable to establish colonies on WT plants, but five adult aphids grew to colonies averaging > 30 aphids after 9 d on both mutant lines (Fig. 5e; Table S15; Kruskal–Wallis, $H_2 = 24.37$, $P < 0.001$, Wilcoxon rank-sum with Bonferroni correction: WT-*cyp87a126-1* $P < 0.001$, WT-*cyp87a126-2* $P < 0.001$, *cyp87a126-1*-*cyp87a126-2*: $P = 0.76$). None of the 14 *P. rapae* caterpillars placed on WT plants began feeding, while 29 of 30 caterpillars placed on the two mutant lines fed and produced substantial damage (Figs 5f, S5; Table S16; $\chi^2 = 39.8$, df = 2, $P < 0.001$). While mortality of *P. rapae* caterpillars was high, four of those feeding on mutant plants reached pupation, demonstrating their suitability as a host plant.

Herbivore attack in the field

On plants growing in the field, a total of 2435 visitors from 30 distinct functional or taxonomic groups were recorded on *E. cheiranthoides* WT, *cyp87a126-1*, and *cyp87a126-2* across four censuses spanning 1 month. We removed some plants from the analysis due to suspected mammalian herbivore damage (WT: 8 of 60, *cyp87a126-1*: 3 of 30, and *cyp87a126-2*: 6 of 30), which was not biased toward any genotype ($\chi^2 = 1.302$, df = 2, $P = 0.52$). Rare visitors, defined as appearing on fewer than 25

© 2024 The Authors
New Phytologist © 2024 New Phytologist Foundation

14698137, 0, Downloaded from https://nph.onlinelibrary.wiley.com/doi/10.1111/nph.19534 by Cornell University, Wiley Online Library on [03/03/2024]. See the Terms and Conditions (https://onlinelibrary.wiley.com/terms-and-conditions) on Wiley Online Library for rules of use; OA articles are governed by the applicable Creative Commons License

unique plants (24% of all plants) across the four censuses, were not subjected to statistical analysis. Common visitors included striped flea beetles (*Phyllotreta striolata* F.), turnip aphids (*Lipaphis erysimi* Kaltenbach), leafhoppers, snails, spiders, leaf miners, and *P. rapae* eggs. Snails of the family Succineidae were less likely to be found on WT plants (WT observation rate: 0.44, 95% CI 0.31–0.058, $P = 0.41$) than on *cyp87a126-1* plants (*cyp87a126-1* observation rate: 0.74, 95% CI 0.55–0.87, $P = 0.013$) or *cyp87a126-2* plants (*cyp87a126-2* observation rate: 0.92, 95% CI 0.72–0.98, $P < 0.001$; Fig. 6c). Similarly, *P. rapae* eggs were more likely to be found on either mutant line than on WT plants (Fig. 6d; WT observation rate: 0.04, 95% CI 0.01–

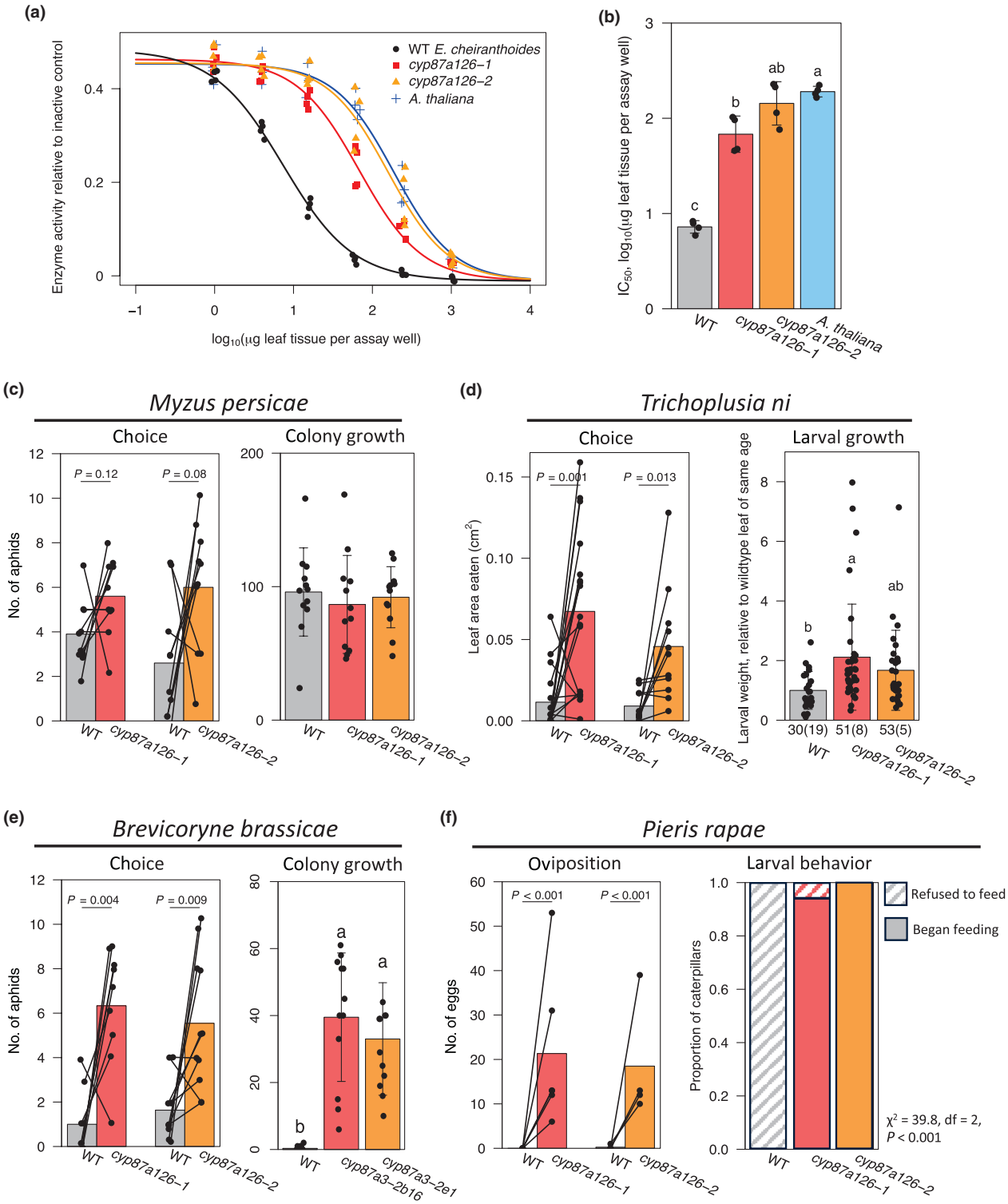

© 2024 The Authors
New Phytologist © 2024 New Phytologist Foundation

14698137, 0, Downloaded from https://nph.onlinelibrary.wiley.com/doi/10.1111/nph.19534 by Cornell University, Wiley Online Library on [03/03/2024]. See the Terms and Conditions (https://onlinelibrary.wiley.com/terms-and-conditions) on Wiley Online Library for rules of use; OA articles are governed by the applicable Creative Commons License

Fig. 5 Functional implications of *Erysimum cheiranthoides cyp87a126* knockout and loss of cardiac glycosides. (a) Na^+,K^+-ATPase inhibition assay for leaf extracts of *cyp87a126* mutant lines compared with wildtype (WT) *E. cheiranthoides* and *Arabidopsis thaliana* Col-0 as a cardiac glycoside-free control. Inhibition curves were calculated from four replicates of each tissue. (b) Half-maximal inhibitory concentration of leaf extracts estimated from inflection point of inhibition curves ($n = 4$ plants per line). (c, e) *Myzus persicae* and *Brevicoryne brassicae* aphid assays: binary choice as measured by aphid position after 24 h ($n = 10$ aphids per replicate, 9–11 replicates per line); colony growth of five synchronized aphids after 9 d ($n = 12$ plants per line). (d) *Trichoplusia ni* assays: binary choice, leaf area eaten after 2 d ($n = 18$); growth, larval weight after 12 d of feeding, normalized by leaf position to remove the effect of leaf age ($n = 25$–37 caterpillars per line). Numbers below plot indicate caterpillars surviving or dying (in parentheses) after 8 d. (f) *Pieris rapae* assays: oviposition in binary choice assay ($n = 75$–128 eggs); larval behavior when confined to an individual leaf ($n = 13$–17 caterpillars). For all plots: error bars indicate ±SD; letters indicate statistical differences ($P < 0.05$) according to a one-way ANOVA with a *post hoc* Tukey's HSD, except for (e), where a Kruskal–Wallis test with pairwise Wilcoxon rank-sum comparisons was used. *P*-values are from paired *t*-tests in choice assays or chi-squared test in oviposition and larval behavior assays.

0.14, $P < 0.001$; *cyp87a126-1* observation rate: 0.48, 95% CI 0.30–0.66, $P < 0.001$; *cyp87a126-2* observation rate: 0.45, 0.27–0.65, $P < 0.001$). Visitation rates did not differ between WT and *cyp87a126* mutant lines for *P. striolata* (Fig. 6a; one-way ANOVA: $F_{2,97} = 2.23$, $P = 0.11$), *L. erysimi* (Fig. 6b; WT observation rate: 0.32, 95% CI 0.21–0.46, $P = 0.01$; *cyp87a126-1* observation rate: 0.48, 95% CI 0.30–0.66, $P = 0.18$; *cyp87a126-2* observation rate: 0.21, 0.09–0.41, $P < 0.29$), leafhoppers, leaf miners, or spiders. Complete visitation records and results of all logistic regressions are in Tables S17 and S18, respectively.

Discussion

Convergent evolution of CYP87A126 as a sterol side-chain cleaving enzyme and the first committed step in cardiac glycoside biosynthesis

The presence of sterol side-chain cleaving enzymes in cardiac glycoside-producing plants has been the subject of speculation for decades (Stohs & El-Olemy, 1971; Pilgrim, 1972; Lindemann & Luckner, 1997; Iino *et al.*, 2007; Lindemann, 2015),

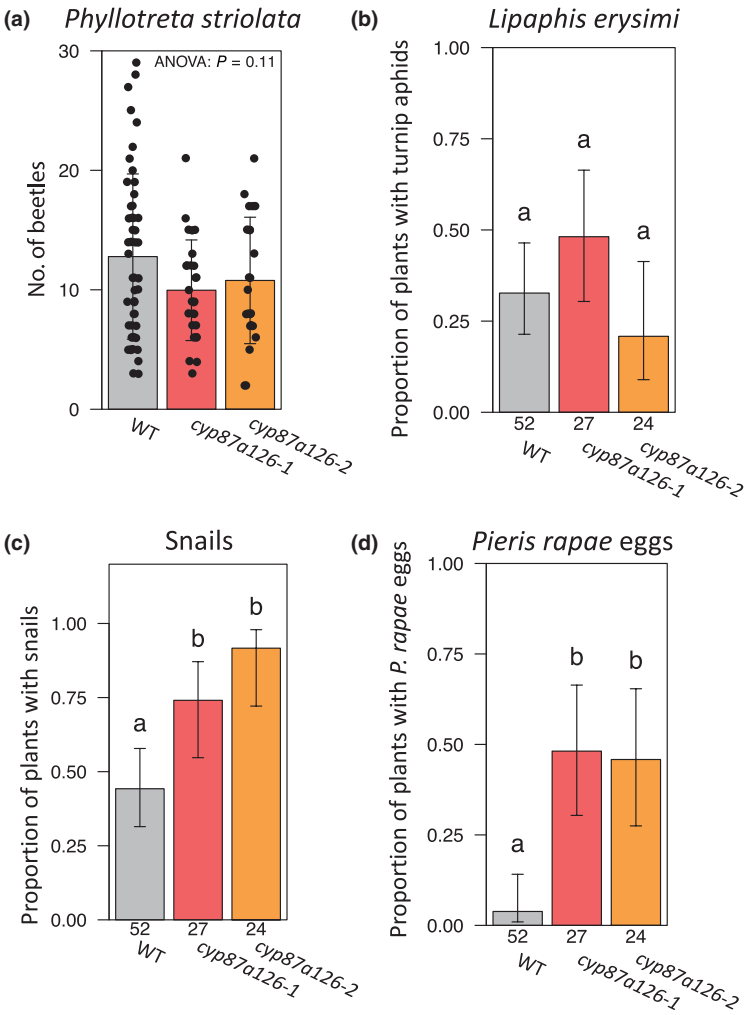

Fig. 6 Observation rates of common visitors across four censuses in a field setting. (a) Count of flea beetles (*Phyllotreta striolata*) on each plant during the fourth census, when they were most abundant. Error bars indicate ±SD. Proportion of plants with (b) turnip aphid (*Lipaphis erysimi*), (c) snails of the family Succineidae, or (d) cabbage butterfly (*Pieris rapae*) eggs at any point across the four censuses. Numbers below bars indicate the number of surviving plants belonging to each genotype that were included in the analysis. For (b–d), error bars indicate 95% confidence interval from logistic regression, and letters denote differences between estimated marginal means for each group, Tukey-adjusted $P < 0.05$.

© 2024 The Authors
New Phytologist © 2024 New Phytologist Foundation

14698137, 0, Downloaded from https://nph.onlinelibrary.wiley.com/doi/10.1111/nph.19534 by Cornell University, Wiley Online Library on [03/03/2024]. See the Terms and Conditions (https://onlinelibrary.wiley.com/terms-and-conditions) on Wiley Online Library for rules of use; OA articles are governed by the applicable Creative Commons License

14698137, 0, Downloaded from https://nph.onlinelibrary.wiley.com/doi/10.1111/nph.19534 by Cornell University, Wiley Online Library on [03/03/2024]. See the Terms and Conditions (https://onlinelibrary.wiley.com/terms-and-conditions) on Wiley Online Library for rules of use; OA articles are governed by the applicable Creative Commons License

and they have only recently been identified in *Digitalis* spp., *Calotropis procera*, and *E. cheiranthoides* (Carroll *et al.*, 2023; Kunert *et al.*, 2023). In this study, we independently confirm that *Ec*CYP87A126 possesses sterol side-chain cleaving activity and generate knockout lines showing that this activity is required for cardiac glycoside production *in planta*. This discovery is an important first step toward establishing the full cardiac glycoside biosynthetic pathway in *Erysimum*. Based on substrate feeding experiments, it is now clear that *Erysimum* cardiac glycoside biosynthesis proceeds through pregnane intermediates, much like in *Digitalis* (Kunert *et al.*, 2023). Notably, the two amino acid substitutions identified by Carroll *et al.* (2023) that are necessary for sterol side-chain cleaving activity in *Dl*CYP87A4, V355A, and A357L, are also present in *Ec*CYP87A126. While the ancestral function of the CYP87A clade is unknown, other related enzymes are known to act on triterpenoids (Zhou *et al.*, 2016; Ghosh, 2017).

A second cytochrome P450 involved in cardiac glycoside biosynthesis

Our screen of cytochrome P450 monooxygenases revealed a second P450 that is involved in cardiac glycoside modification. Ec*CYP716A418* mutant lines make high quantities of cardiac glycosides, but they almost exclusively accumulate digitoxigenin glycosides, which are not oxygenated at carbons 4 and 19 (Fig. 1). Based on the predicted pathway, we hypothesize that *Ec*CYP716A418 hydroxylates digitoxigenin at carbon 19. However, we did not see this activity when co-infiltrating *Ec*CYP716A418 with digitoxigenin or digitoxin in *N. benthamiana*. This result leaves open the possibility that hydroxylation by *Ec*CYP716A418 occurs earlier in the pathway, for example before lactone ring formation. It is also possible that the observed phenotype is somewhat more cryptic, and there is no direct link between this enzyme and cardiac glycoside hydroxylation. Other members of the CYP716A family are well known for the modification of triterpenoid scaffolds, including β-amyrin (Carelli *et al.*, 2011; Yasumoto *et al.*, 2016; Ghosh, 2017). In addition, Ec*CYP716A418* is duplicated several times in *E. cheiranthoides* relative to *A. thaliana* (Fig. 2d), a pattern that is often observed in the evolution of specialized metabolic pathways (Moghe & Last, 2015).

A knockout line of the third cytochrome P450 discussed in this paper, Ec*CYP71B132*, did not have an altered cardiac glycoside phenotype. The lack of a phenotype does not conclusively exclude the involvement of *Ec*CYP71B132 in cardiac glycoside biosynthesis. For example, a potential alternative start codon 50 base pairs after the Cas9-induced deletion may result in a functional protein with an *N*-terminal truncation of 66 amino acids. Even if *cyp71b132-1* is a complete functional knockout, it is possible that its role in cardiac glycoside biosynthesis is complemented by a functionally redundant enzyme. Nonetheless, the lack of known CYP71B family members acting on steroid-like compounds indicates that the involvement of *Ec*CYP71B132 in cardiac glycoside biosynthesis is less likely. Rather, the most closely related characterized enzymes act on indolic compounds (Böttcher *et al.*, 2009, 2014).

Cardiac glycosides as escape from herbivory

While it has long been understood that *Erysimum* represents a unique instance of the co-occurrence of two potent defensive compounds (Züst *et al.*, 2018), the overall benefit of investing in two distinct but potentially redundant defenses has been difficult to test. Ec*CYP87A126* mutant lines lacked the Na^+/K^+-ATPase inhibitory activity associated with cardiac glycosides *in vitro*, but our insect performance assays and field experiment highlight that plant–insect relationships can be highly species-specific. In the laboratory, generalist *M. persicae* aphids performed similarly on *E. cheiranthoides* regardless of the presence of cardiac glycosides, and generalist *T. ni* caterpillars preferred the cardiac glycoside-free mutant but grew only slightly better when feeding on it. This is perhaps unsurprising as generalist insects are known for their ability to tolerate a wide range of defensive metabolites. Nevertheless, previous studies have demonstrated that cardiac glycosides from *Asclepias curassavica* latex are acutely toxic to *T. ni* caterpillars (Dussourd & Hoyle, 2000), so additional factors likely play a role, including the concentration and chemical structure of cardiac glycosides produced. Conversely, we found that snails from the family Succineidae, which are also broad generalists, were more likely to be found on cardiac glycoside-free mutant plants in the field. Although we did not quantify damage caused by snails, this agrees with previous work showing that cardiac glycosides can be effective molluscicides (Dai *et al.*, 2011). This apparently variable effect of cardiac glycosides on generalist herbivores suggests that they do not allow uniform escape from herbivory but may instead result in more subtle shifts in context-dependent manner.

A much clearer impact of the loss of cardiac glycosides is the reversal of *Erysimum*'s escape from herbivory by two glucosinolate-feeding specialist herbivores. Consistent with previous reports (Rothschild *et al.*, 1988; Renwick *et al.*, 1989; Sachdev-Gupta *et al.*, 1993), we found that both *P. rapae* and *B. brassicae* are unable to utilize WT *E. cheiranthoides* as a host plant. However, with the loss of cardiac glycoside biosynthesis in the Ec*CYP87A126* mutant lines, *P. rapae* found *E. cheiranthoides* to be an acceptable host in both field and laboratory settings, and *B. brassicae* aphids established robust colonies in the laboratory. This greater sensitivity of these crucifer specialists to cardiac glycosides is consistent with a theory proposed by Cornell and Hawkins (2003), who concluded that specialist insect herbivores are less likely to tolerate novel defensive compounds like cardiac glycosides in *Erysimum*. However, two crucifer specialists observed in the field, *P. striolata* and *L. erysimi*, did not show a preference for cardiac glycoside-free *E. cheiranthoides*.

The complete escape from even a subset of specialist insects would represent a distinct ecological advantage, as specialist insects are observed to cause the majority of damage a plant suffers in certain contexts (Coley & Barone, 1996; Bidart-Bouzat & Kliebenstein, 2008). Despite this apparently clear defensive advantage, cardiac glycoside production has been lost or drastically reduced in the accession of *E. collinum* screened in this study (Züst *et al.*, 2020). Whether this loss has become fixed would require more thorough sampling in its native range in Iran, but the persistence of even some individuals with a complete lack of

© 2024 The Authors
New Phytologist © 2024 New Phytologist Foundation

14698137, 0, Downloaded from https://nph.onlinelibrary.wiley.com/doi/10.1111/nph.19534 by Cornell University, Wiley Online Library on [03/03/2024]. See the Terms and Conditions (https://onlinelibrary.wiley.com/terms-and-conditions) on Wiley Online Library for rules of use; OA articles are governed by the applicable Creative Commons License

cardiac glycosides points to context-dependent benefits and likely substantial costs of cardiac glycoside production. *Erysimum collinum* also accumulates high levels of glucoerypestrin, a glucosinolate unique to *Erysimum* (Kjær & Gmelin, 1957; Fahey *et al.*, 2001; Blažević *et al.*, 2020; Züst *et al.*, 2020) that may have allowed an alternative escape route from glucosinolate specialists, rendering cardiac glycosides unnecessary as a second line of defense. By contrast, there are no known cases of the loss of glucosinolates in *Erysimum*, perhaps because glucosinolates are involved in nondefensive processes such as signaling and development (Katz *et al.*, 2015). Within this context, it is important to consider not just the presence or absence of a given chemical class but also variation of chemical structure and toxicity within each class. In *Erysimum*, any defensive advantage afforded by cardiac glycosides may be contingent upon the underlying glucosinolate profile, and vice versa. In order to more fully dissect the interplay between glucosinolates and cardiac glycosides in insect defense and plant fitness, we will generate additional *E. cheiranthoides* mutant lines deficient in indole and/or aliphatic glucosinolates. Field trials with these mutant lines will allow more robust inferences about *Erysimum*'s escape from herbivory and the potential tradeoffs between cardiac glycosides, glucosinolates, growth, and fitness.

Acknowledgements

We thank Prof. Tobias Züst for his insightful comments on the manuscript, Prof. David Nelson for cytochrome P450 naming, Julia Dahl for her assistance with insect experiments, and Dr Boaz Negin for assistance with the field trial. This research was funded by the United States Department of Agriculture award 2020-67013-30896 and an award from the Triad Foundation to GJ; a Chemistry-Biology Interface Training Program fellowship under the National Institutes of Health/National Institute of General Medical Sciences (T32GM138826) and a US National Science Foundation Graduate Research Fellowship (DGE–2139899) to GCY; a Summer Undergraduate Research Fellowship from the American Society of Plant Biologists and a Rawlings Cornell Presidential Research Scholar award to MLA; and a fellowship from the Cane-Bridge Foundation to APC.

Competing interests

None declared.

Author contributions

GCY, MLA, HDF, MM and GJ designed the research. GCY, MLA, HDF, MM, APC and APH performed the research. GCY and MLA analyzed the data. GCY, AAA and GJ wrote and edited the manuscript.

ORCID

Anurag A. Agrawal https://orcid.org/0000-0003-0095-1220
Martin L. Alani https://orcid.org/0000-0002-1356-9760
Georg Jander https://orcid.org/0000-0002-9675-934X
Anamaría Páez-Capador https://orcid.org/0009-0004-7960-3548
Gordon C. Younkin https://orcid.org/0000-0002-3735-3534

Data availability

The data that support the findings of this study are available in the Supporting Information. Raw sequencing reads are publicly available on NCBI (PRJNA1015726). Seeds from mutant lines are available from the Arabidopsis Biological Resource Center (https://abrc.osu.edu/): *cyp87a126-1* (CS29906), *cyp87a126-2* (CS29907), *cyp716a418-1* (CS29908), *cyp716a418-2* (CS29909), and *cyp71b132-1* (CS29910).

References

Alani ML, Younkin GC, Mirzaei M, Kumar P, Jander G. 2021. Acropetal and basipetal cardenolide transport in *Erysimum cheiranthoides* (wormseed wallflower). *Phytochemistry* **192**: 112965.

Bach SS, Bassard J-É, Andersen-Ranberg J, Møldrup ME, Simonsen HT, Hamberger B. 2014. High-throughput testing of terpenoid biosynthesis candidate genes using transient expression in *Nicotiana benthamiana*. In: Rodríguez-Concepción M, ed. *Plant isoprenoids: methods and protocols*. New York, NY, USA: Springer New York, 245–255.

Bidart-Bouzat MG, Kliebenstein DJ. 2008. Differential levels of insect herbivory in the field associated with genotypic variation in glucosinolates in *Arabidopsis thaliana*. *Journal of Chemical Ecology* **34**: 1026–1037.

Blažević I, Montaut S, Burčul F, Olsen CE, Burow M, Rollin P, Agerbirk N. 2020. Glucosinolate structural diversity, identification, chemical synthesis and metabolism in plants. *Phytochemistry* **169**: 112100.

Böttcher C, Chapman A, Fellermeier F, Choudhary M, Scheel D, Glawischnig E. 2014. The biosynthetic pathway of indole-3-carbaldehyde and indole-3-carboxylic acid derivatives in Arabidopsis. *Plant Physiology* **165**: 841–853.

Böttcher C, Westphal L, Schmotz C, Prade E, Scheel D, Glawischnig E. 2009. The multifunctional enzyme CYP71b15 (PHYTOALEXIN DEFICIENT3) converts cysteine-indole-3-acetonitrile to camalexin in the indole-3-acetonitrile metabolic network of *Arabidopsis thaliana*. *Plant Cell* **21**: 1830–1845.

Bray NL, Pimentel H, Melsted P, Pachter L. 2016. Near-optimal probabilistic RNA-seq quantification. *Nature Biotechnology* **34**: 525–527.

Brock A, Herzfeld T, Paschke R, Koch M, Dräger B. 2006. Brassicaceae contain nortropane alkaloids. *Phytochemistry* **67**: 2050–2057.

Carelli M, Biazzi E, Panara F, Tava A, Scaramelli L, Porceddu A, Graham N, Odoardi M, Piano E, Arcioni S *et al.* 2011. *Medicago truncatula* CYP716A12 is a multifunctional oxidase involved in the biosynthesis of hemolytic saponins. *Plant Cell* **23**: 3070–3081.

Carroll E, Gopal BR, Raghavan I, Mukherjee M, Wang ZQ. 2023. A cytochrome P450 CYP87A4 imparts sterol side-chain cleavage in digoxin biosynthesis. *Nature Communications* **14**: 4042.

Clough SJ, Bent AF. 1998. Floral dip: a simplified method for Agrobacterium-mediated transformation of *Arabidopsis thaliana*. *The Plant Journal* **16**: 735–743.

Coley PD, Barone JA. 1996. Herbivory and plant defenses in tropical forests. *Annual Review of Ecology and Systematics* **27**: 305–335.

Cornell HV, Hawkins BA. 2003. Herbivore responses to plant secondary compounds: a test of phytochemical coevolution theory. *American Naturalist* **161**: 507–522.

Dai L, Wang W, Dong X, Hu R, Nan X. 2011. Molluscicidal activity of cardiac glycosides from *Nerium indicum* against *Pomacea canaliculata* and its implications for the mechanisms of toxicity. *Environmental Toxicology and Pharmacology* **32**: 226–232.

Dong L, Almeida A, Pollier J, Khakimov B, Bassard JE, Miettinen K, Stærk D, Mehran R, Olsen CE, Motawia MS *et al.* 2021. An independent evolutionary

© 2024 The Authors
New Phytologist © 2024 New Phytologist Foundation

origin for insect deterrent cucurbitacins in *Iberis amara*. *Molecular Biology and Evolution* **38**: 4659–4673.

Dussourd DE, Hoyle AM. 2000. Poisoned plusiines: toxicity of milkweed latex and cardenolides to some generalist caterpillars. *Chemoecology* **10**: 11–16.

Edger PP, Heidel-Fischer HM, Bekaert M, Rota J, Glöckner G, Platts AE, Heckel DG, Der JP, Wafula EK, Tang M *et al.* 2015. The butterfly plant arms-race escalated by gene and genome duplications. *Proceedings of the National Academy of Sciences, USA* **112**: 8362–8366.

Ehrlich PR, Raven PH. 1964. Butterflies and plants: a study in coevolution. *Evolution* **18**: 586–608.

Fahey JW, Zalcmann AT, Talalay P. 2001. The chemical diversity and distribution of glucosinolates and isothiocyanates among plants. *Phytochemistry* **56**: 5–51.

Feeny P. 1977. Defensive ecology of the Cruciferae. *Annals of the Missouri Botanical Garden* **64**: 221–234.

Feng H, Chen W, Hussain S, Shakir S, Tzin V, Adegbayi F, Ugine T, Fei Z, Jander G. 2023. Horizontally transferred genes as RNA interference targets for aphid and whitefly control. *Plant Biotechnology Journal* **21**: 754–768.

Fraenkel G. 1959. The Raison d'Etre of secondary plant substances. *Science* **129**: 1466–1470.

Frisch T, Møller BL. 2012. Possible evolution of alliarinoside biosynthesis from the glucosinolate pathway in *Alliaria petiolata*. *FEBS Journal* **279**: 1545–1562.

Gatto L, Gibb S, Rainer J. 2020. MSnbase, efficient and elegant R-based processing and visualisation of raw mass spectrometry data. *bioRxiv*. doi: 10.1101/2020.04.29.067868.

Gatto L, Lilley K. 2012. MSNBASE – an R/Bioconductor package for isobaric tagged mass spectrometry data visualization, processing and quantitation. *Bioinformatics* **28**: 288–289.

Getman-Pickering ZL, Campbell A, Aflitto N, Grele A, Davis JK, Ugine TA. 2020. LeafByte: a mobile application that measures leaf area and herbivory quickly and accurately. *Methods in Ecology and Evolution* **11**: 215–221.

Ghosh S. 2017. Triterpene structural diversification by plant cytochrome P450 enzymes. *Frontiers in Plant Science* **8**: 1–15.

Gordon HT. 1961. Nutritional factors in insect resistance to chemicals. *Annual Review of Entomology* **6**: 27–54.

Graves S, Piepho H-P, with help from Sundar Dorai-Raj LS. 2023. *MULTCOMPVIEW*: *visualizations of paired comparisons*.

Hoang DT, Chernomor O, Von Haeseler A, Minh BQ, Vinh LS. 2018. UFBOOT2: improving the ultrafast bootstrap approximation. *Molecular Biology and Evolution* **35**: 518–522.

Iino M, Nomura T, Tamaki Y, Yamada Y, Yoneyama K, Takeuchi Y, Mori M, Asami T, Nakano T, Yokota T. 2007. Progesterone: its occurrence in plants and involvement in plant growth. *Phytochemistry* **68**: 1664–1673.

Katz E, Nisani S, Sela M, Behar H, Chamovitz DA, Katz E, Nisani S, Sela M, Behar H, Chamovitz DA. 2015. The effect of indole-3-carbinol on PIN1 and PIN2 in Arabidopsis roots. *Plant Signaling and Behavior* **2324**: 16–19.

Kjær A, Gmelin R. 1957. isoThiocyanates XXV. Methyl 4-isoThiocyanatobutyrate, a new mustard oil present as a glucoside (Glucoerypestrin) in *Erysimum* species. *Acta Chemica Scandinavica* **11**: 577–578.

Kunert M, Langley C, Lucier R, Ploss K, Rodríguez López CE, Serna Guerrero DA, Rothe E, O'Connor SE, Sonawane PD. 2023. Promiscuous CYP87A enzyme activity initiates cardenolide biosynthesis in plants. *Nature Plants* **9**: 1607–1617.

Lenth RV. 2023. *EMMEANS*: *estimated marginal means, aka least-squares means*. R package v.1.8.9. [WWW document] URL https://CRAN.R-project.org/package=emmeans [accessed 2 November 2023].

Lindemann P. 2015. Steroidogenesis in plants – biosynthesis and conversions of progesterone and other pregnane derivatives. *Steroids* **103**: 145–152.

Lindemann P, Luckner M. 1997. Biosynthesis of pregnane derivatives in somatic embryos of *Digitalis lanata*. *Phytochemistry* **46**: 507–513.

Madeira F, Pearce M, Tivey ARN, Basutkar P, Lee J, Edbali O, Madhusoodanan N, Kolesnikov A, Lopez R. 2022. Search and sequence analysis tools services from EMBL-EBI in 2022. *Nucleic Acids Research* **50**: W276–W279.

Makarevich IF, Zhernoklev KV, Slyusarskaya TV, Yarmolenko GN. 1994. Cardenolide-containing plants of the family Cruciferae. *Chemistry of Natural Compounds* **30**: 275–289.

McCarthy DJ, Chen Y, Smyth GK. 2012. Differential expression analysis of multifactor RNA-Seq experiments with respect to biological variation. *Nucleic Acids Research* **40**: 4288–4297.

Minh BQ, Schmidt HA, Chernomor O, Schrempf D, Woodhams MD, Von Haeseler A, Lanfear R, Teeling E. 2020. IQ-TREE 2: new models and efficient methods for phylogenetic inference in the genomic era. *Molecular Biology and Evolution* **37**: 1530–1534.

Moghe G, Last RL. 2015. Something old, something new: conserved enzymes and the evolution of novelty in plant specialized metabolism. *Plant Physiology* **169**: 1512–1523.

Monroe JG. 2017. *GENEMODEL*: *gene model plotting in R*. R package v.1.1.0, [WWW document] URL https://CRAN.R-project.org/package=genemodel [accessed 18 April 2023].

Nielsen J. 1978a. Host plant discrimination within Cruciferae: feeding responses of four leaf beetles (Coleoptera: Chrysomelidae) to glucosinolates, cucurbitacins and cardenolides. *Entomologia Experimentalis et Applicata* **24**: 41–54.

Nielsen J. 1978b. Host plant selection of monophagous and oligophagous flea beetles feeding on crucifers. *Entomologia Experimentalis et Applicata* **24**: 362–369.

Okamura Y, Dort H, Reichelt M, Tunstrom K, Wheat CW, Vogel H. 2022. Testing hypotheses of a coevolutionary key innovation reveals a complex suite of traits involved in defusing the mustart oil bomb. *Proceedings of the National Academy of Sciences, USA* **119**: e2208447119.

Petschenka G, Züst T, Hastings AP, Agrawal AA, Jander G. 2023. Quantification of plant cardenolides by HPLC, measurement of Na+/K+-ATPase inhibition activity, and characterization of target enzymes. *Methods in Enzymology* **680**: 275–302.

Pilgrim H. 1972. 'Cholesterol side-chain cleaving enzyme' aktivität in keimlingen und *in vitro* kultivierten geweben von *Digitalis purpurea*. *Phytochemistry* **11**: 1725–1728.

Pinheiro J, Bates D. 2000. *Mixed-effects models in S and S-PLUS*. New York, NY, USA: Springer.

Pinheiro J, Bates D. 2023. *NLME*: *linear and nonlinear mixed effects models*. R package v.3.1-164. [WWW document] URL https://CRAN.R-project.org/package=nlme [accessed 2 November 2023].

R Core Team. 2020. *R: a language and environment for statistical computing*. Vienna, Austria: R Foundation for Statistical Computing.

Ramsey JS, Elzinga DA, Sarkar P, Xin YR, Ghanim M, Jander G. 2014. Adaptation to nicotine feeding in *Myzus persicae*. *Journal of Chemical Ecology* **40**: 869–877.

Ramsey JS, Wilson ACC, de Vos M, Sun Q, Tamborindeguy C, Winfield A, Malloch G, Smith DM, Fenton B, Gray SM *et al.* 2007. Genomic resources for *Myzus persicae*: EST sequencing, SNP identification, and microarray design. *BMC Genomics* **8**: 423.

Renwick J, Radke C, Sachdev-Gupta K. 1989. Chemical consituents of *Erysimum cheiranthoides* deterring oviposition by cabbage butterfly, *Pieris rapae*. *Journal of Chemical Ecology* **15**: 2161–2169.

Robinson MD, McCarthy DJ, Smyth GK. 2010. EDGER: a bioconductor package for differential expression analysis of digital gene expression data. *Bioinformatics* **26**: 139–140.

Rothschild M, Alborn H, Stenhagen G, Schoonhoven LM. 1988. A strophanthidin glycoside in siberian wallflower: a contact deterrent for the large white butterfly. *Phytochemistry* **27**: 101–108.

Sachdev-Gupta K, Radke C, Renwick JAA, Dimock MB. 1993. Cardenolides from *Erysimum cheiranthoides*: feeding deterrents to *Pieris rapae* larvae. *Journal of Chemical Ecology* **19**: 1355–1369.

Sainsbury F, Thuenemann EC, Lomonossoff GP. 2009. PEAQ: versatile expression vectors for easy and quick transient expression of heterologous proteins in plants. *Plant Biotechnology Journal* **7**: 682–693.

Shinoda T, Nagao T, Nakayama M, Serizawa H, Koshioka M, Okabe H, Kawai A. 2002. Identification of a triterpenoid saponin from a crucifer, *Barbarea vulgaris*, as a feeding deterrent to the diamondback moth, *Plutella xylostella*. *Journal of Chemical Ecology* **28**: 587–599.

Sievers F, Wilm A, Dineen D, Gibson TJ, Karplus K, Li W, Lopez R, McWilliam H, Remmert M, Söding J *et al.* 2011. Fast, scalable generation of high-quality protein multiple sequence alignments using Clustal Omega. *Molecular Systems Biology* **7**: 539.

© 2024 The Authors
New Phytologist © 2024 New Phytologist Foundation

14698137, 0, Downloaded from https://nph.onlinelibrary.wiley.com/doi/10.1111/nph.19534 by Cornell University, Wiley Online Library on [03/03/2024]. See the Terms and Conditions (https://onlinelibrary.wiley.com/terms-and-conditions) on Wiley Online Library for rules of use; OA articles are governed by the applicable Creative Commons License

Stohs SJ, El-Olemy MM. 1971. Pregnenolone and progesterone from 20a-hydroxycholesterol by *Cheiranthus cheiri* leaf homogenates. *Phytochemistry* **10**: 3053–3056.

Strickler SR, Powell AF, Mueller LA, Zust T, Jander G. 2019. NCBI BioProject ID PRJNA563696. *Rapid and independent evolution of ancestral and novel chemical defenses in a genus of toxic plants (Erysimum, Brassicaceae)*.

Thompson JN. 1989. Concepts of coevolution. *Trends in Ecology and Evolution* **4**: 179–183.

Trifinopoulos J, Nguyen LT, von Haeseler A, Minh BQ. 2016. W-IQ-TREE: a fast online phylogenetic tool for maximum likelihood analysis. *Nucleic Acids Research* **44**: W232–W235.

Wang WC, Menon G, Hansen G. 2003. Development of a novel *Agrobacterium*-mediated transformation method to recover transgenic *Brassica napus* plants. *Plant Cell Reports* **22**: 274–281.

Weigel D, Glazebrook J. 2006. Transformation of agrobacterium using the freeze-thaw method. *CSH Protocols* **7**: pdb.prot4666.

Wisecaver JH, Borowsky AT, Tzin V, Jander G, Kliebenstein DJ, Rokas A. 2017. A global coexpression network approach for connecting genes to specialized metabolic pathways in plants. *Plant Cell* **29**: 944–959.

Yasumoto S, Fukushima EO, Seki H, Muranaka T. 2016. Novel triterpene oxidizing activity of *Arabidopsis thaliana* CYP716A subfamily enzymes. *FEBS Letters* **590**: 533–540.

Zhong S, Joung JG, Zheng Y, Chen YR, Liu B, Shao Y, Xiang JZ, Fei Z, Giovannoni JJ. 2011. High-throughput illumina strand-specific RNA sequencing library preparation. *Cold Spring Harbor Protocols* **6**: 940–949.

Zhou Y, Ma Y, Zeng J, Duan L, Xue X, Wang H, Lin T, Liu Z, Zeng K, Zhong Y *et al.* 2016. Convergence and divergence of bitterness biosynthesis and regulation in Cucurbitaceae. *Nature Plants* **2**: 1–8.

Züst T, Mirzaei M, Jander G. 2018. *Erysimum cheiranthoides*, an ecological research system with potential as a genetic and genomic model for studying cardiac glycoside biosynthesis. *Phytochemistry Reviews* **17**: 1239–1251.

Züst T, Strickler SR, Powell AF, Mabry ME, An H, Mirzaei M, York T, Holland CK, Kumar P, Erb M *et al.* 2020. Independent evolution of ancestral and novel defenses in a genus of toxic plants (Erysimum, Brassicaceae). *eLife* **9**: 1–42.

Supporting Information

Additional Supporting Information may be found online in the Supporting Information section at the end of the article.

Fig. S1 Maps for plasmids used to generate Cas9 constructs.

Fig. S2 Experimental setup for insect assays.

Fig. S3 Gene models for Cas9 targets and knockout lines.

Fig. S4 Photographs of leaf disks from *Trichoplusia ni* choice assay.

Fig. S5 Photographs of leaves from *Pieris rapae* feeding assay.

Table S1 Sequences for primers used in this study.

Table S2 *m/z* Values and retention times used for quantifying cardiac glycosides in LCMS data.

Table S3 *m/z* Values and retention times used for quantifying glucosinolates in LCMS data.

Table S4 Full-length coding sequences for cytochrome P450s.

Table S5 Relative peak area for *cyp716a418* cardiac glycosides.

Table S6 Relative peak area for *cyp87a126* cardiac glycosides.

Table S7 Relative peak area for *cyp87a126* glucosinolates.

Table S8 Raw data from Na^+,K^+-ATPase assay.

Table S9 Raw data from *Myzus persicae* choice assay.

Table S10 Raw data from *Trichoplusia ni* choice assay.

Table S11 Raw data from *Brevicoryne brassicae* choice assay.

Table S12 Raw data from *Pieris rapae* oviposition assay.

Table S13 Raw data from *Myzus persicae* growth assay.

Table S14 Raw data from *Trichoplusia ni* growth assay.

Table S15 Raw data from *Brevicoryne brassicae* growth assay.

Table S16 Raw data from *Pieris rapae* feeding assay.

Table S17 Complete observation records from the field experiment.

Table S18 Logistic regressions for common taxa in the field experiment.

Please note: Wiley is not responsible for the content or functionality of any Supporting Information supplied by the authors. Any queries (other than missing material) should be directed to the *New Phytologist* Central Office.

© 2024 The Authors
New Phytologist © 2024 New Phytologist Foundation

14698137, 0, Downloaded from https://nph.onlinelibrary.wiley.com/doi/10.1111/nph.19534 by Cornell University, Wiley Online Library on [03/03/2024]. See the Terms and Conditions (https://onlinelibrary.wiley.com/terms-and-conditions) on Wiley Online Library for rules of use; OA articles are governed by the applicable Creative Commons License